Doxorubicin Intracellular Remote Release from Biocompatible Oligo(ethylene glycol) Methyl Ether Methacrylate-Based Magnetic Nanogels Triggered by Magnetic Hyperthermia

Esther Cazares-Cortes, Ana Espinosa, Jean-Michel Guigner, Aude Michel, Nébéwia Griffete, Claire Wilhelm, Christine Ménager

Doxorubicin Intracellular Remote Release from Biocompatible OEGMA-based Magnetic Nanogels Triggered by Magnetic Hyperthermia

Esther Cazares-Cortes[a], *Ana Espinosa*[b], *Jean-Michel Guigner*[c], *Aude Michel*[a], *Nébéwia Griffete*[a], *Claire Wilhelm*[b]* *and Christine Ménager*[a]*

[a] Sorbonne Universités, UPMC Univ. Paris 06, CNRS, UMR 8234, Laboratory PHENIX, 4 place Jussieu, F-75005 Paris, France

[b] Univ. Paris Diderot, CNRS, UMR 7057, Laboratory MSC, 75205 Paris cedex 13, France

[c] Sorbonne Universités, UPMC Univ. Paris 06, CNRS, UMR 7590, Laboratory IMPMC, IRD, MNHN, 4 place Jussieu, F-75005 Paris, France

KEYWORDS: oligo(ethylene glycol) methacrylates nanogels, magnetic nanoparticles, magnetic hyperthermia, remote drug release, cancer therapy

ABSTRACT: Hybrid nanogels, composed of thermoresponsive polymers and superparamagnetic nanoparticles (MNPs) are attractive nanocarriers for biomedical applications, being able – as polymer matrix – to uptake and release high quantities of chemotherapeutic agents and – as magnetic nanoparticles – to heat when exposed to an alternative magnetic field (AMF), better known as magnetic hyperthermia. Herein, biocompatible, pH-, magnetic- and thermo-responsive nanogels, based on oligo (ethylene glycol) methacrylate monomers

(OEGMAs) and methacrylic acid co-monomer (MAA) were prepared by conventional precipitation radical co-polymerization in water, post-assembled by complexation with iron oxide magnetic nanoparticles (MNPs) of maghemite (γ-Fe_2O_3) and loaded with an anticancer drug (doxorubicin – DOX), for remotely controlled drug release by "hot-spot", as an athermal magnetic hyperthermia strategy against cancer.

These nanogels, noted MagNanoGels, with a hydrodynamic diameter from 328 to 460 nm, as a function of MNPs content, have a swelling-deswelling behavior at their volume phase temperature transition (VPTT) around 47 °C in a physiological medium (pH 7.5), which is above the human body temperature (37 °C). Applying an alternative magnetic field increases twice the release of DOX, while no macroscopic heating was recorded. This enhanced drug release is due to a shrinking of the polymer network by local heating, as illustrated by the MagNanoGels size decrease under AMF. In cancer cells, not only the DOX-MagNanoGels internalize DOX more efficiently than free DOX, but also DOX intracellular release can be remotely triggered under AMF, in athermal conditions, thus enhancing DOX cytotoxicity.

1. INTRODUCTION

Polymer-based platforms have been widely studied as drug delivery systems (DDS) for cancer therapy, because they can encapsulate high amounts of chemotherapeutic drugs and allow the vectorization of the drug to a given location (tumor). Moreover, depending on the chosen chemical design, the release of the drug can be stimulated by intracellular environmental stimuli such as temperature, pH, redox and/or by an external stimuli: near infrared light (NIR), ultrasounds (US) and alternative magnetic field (AMF).[1–4] Recently, the preparation of smart nanocarriers combining two or more stimuli have attracted scientific attention.[5–7] In particular the combination of pH with another internal / external stimulus is very interesting for cancer

therapy because of the acidic microenvironment of cancerous cells (pH 4.5 – 6.5) compared to physiological microenvironment of normal cells (pH 7.5). Moreover, using an external stimulus may provide control over time and allow regulating the amount of drug release, enhancing therapeutic effectiveness and reducing systemic toxicity. This can be useful in nanomedicine, as the payload can be released on demand. To achieve this goal, researchers have designed hybrid nanodevices containing an organic component such a stimuli responsive and / or biodegradable polymer; and inorganic component such as gold, maghemite, silica nanoparticles (NPs) to form remotely-controlled drug delivery systems (RC-DDS)[8]. These multifunctional hybrid nanodevices can be used, not only as drug carriers, but also as imaging and theranostic agents[5]. More specifically, several RC-DDS based on thermoresponsive polymers and superparamagnetic nanoparticles (MNPs) have been used for remotely trigger drug release by applying AMF: magnetic-thermoresponsive micro/nanogels[9–11], microbeads[12], nanobeads[13], nanocubes[14], polymersomes[15], but most of the time a macroscopic heating of the medium is needed for drug delivery.

Recently, some research groups have demonstrated that polymeric-MNPs nanocarriers (Magnetic Molecularly Imprinted Polymer Nanoparticles[16], polymer coated MNPs[17–19]) can release their payload without macroscopic heating (athermal conditions). In this case, MNPs act as individual “hot spots” and generate a localized heating, i.e. at the nanoscopic scale around the MNPs for triggering the release of the drug, without raising the global temperature. These findings have opened the possibility for the design of new RC-DDS. Thus far, the most studied thermoresponsive polymer in these hybrid nanodevices is the poly(N-isopropylacrylamide) (PNIPAM), but its potential toxicity might limit biomedical applications. Moreover, several studies already indicated that polymers based on oligo(ethylene glycol) methacrylates

(OEGMAs) exhibit an excellent *in vitro* or *in vivo* biocompatibility, such as linear poly(ethylene glycol) polymers[20], which has already been validated by the Food Drug Administration. Hence, nanodevices based on OEGMAs monomers have been elaborated as excellent biocompatible and thermoresponsive nanomaterials[21–25].

Here, we synthetize biocompatible, pH-, magnetic- and thermo-responsive nanogels based on oligo(ethylene glycol) methacrylate (macro)-monomers (OEGMAs) and methacrylic acid co-monomer (MAA), loaded with different mass ratio of γ-Fe_2O_3 superparamagnetic nanoparticles (MNPs – from 9.0 to 66.7 wt%) and doxorubicin (DOX). We propose to trigger the drug release under an alternative magnetic field (AMF) via an athermal magnetic hyperthermia strategy (Scheme 1a-b). The swelling-deswelling behavior of these nanogels, noted MagNanoGels, to various stimuli (temperature, pH and magnetic field) was investigated. Then, in order to demonstrate that MagNanoGels can be used as remotely controlled drug delivery systems (RC-DDS), an important amount of doxorubicin (DOX) was encapsulated into nanogels and their response to pH and to AMF stimuli were analyzed *in vitro* (batch) and in intracellular (PC-3 cancer cells) conditions (scheme 1b).

Scheme 1: Illustration of MagNanoGels synthesis and remotely controlled drug delivery under AMF *

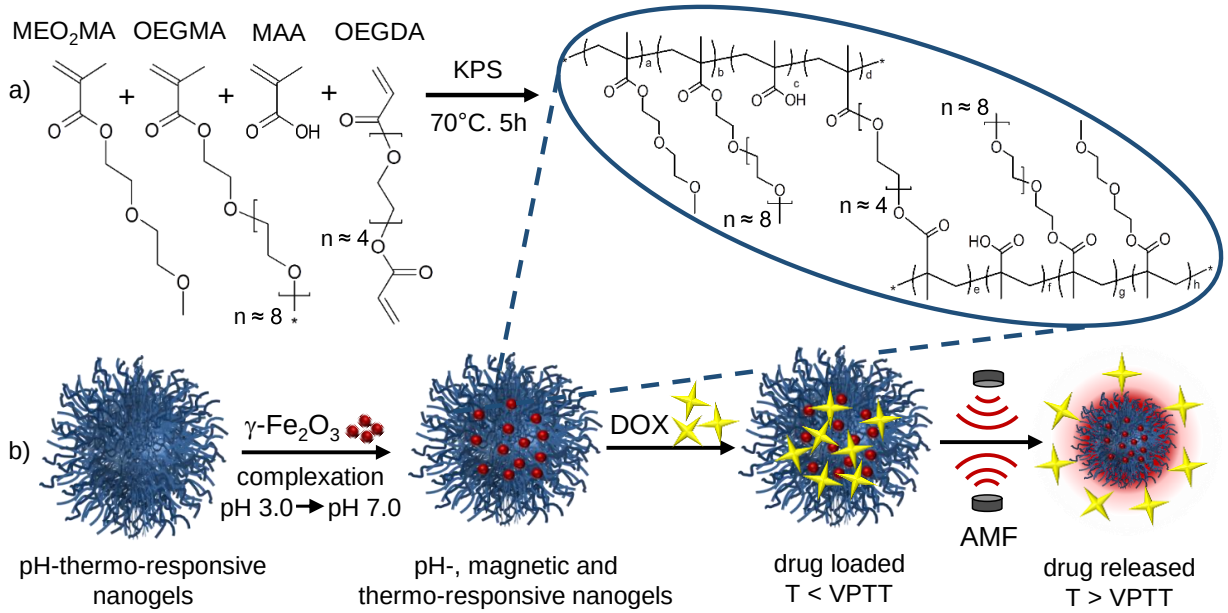

* a) Conventional aqueous precipitation radical co-polymerization reaction of nanogels based on oligo(ethylene glycol) methacrylate monomers. b) Schematic illustration of the MagNanoGels synthesis, loading and release of doxorubicin (DOX) under alternative magnetic field (AMF).

2. EXPERIMENTAL SECTION

2.1 Materials

Iron (II) chloride tetrahydrate ($FeCl_2.4H_2O$), iron (III) chloride hexahydrate ($FeCl_3.6H_2O$), iron (III) nitrate nonahydrate ($Fe(NO_3)_3.9H_2O$), ammonia solution (NH_3, 20 %), nitric acid (HNO_3, 52.5 %) and hydrochloric acid (HCl, 37 %), diethyl ether and technical acetone were purchased from VWR for the preparation of superparamagnetic nanoparticles of maghemite (γ-Fe_2O_3). Poly(ethylene glycol) methyl ether methacrylate (OEGMA, Mn = 500 $g.mol^{-1}$), di(ethylene glycol) methyl ether methacrylate (MEO_2MA, Mn = 188.22 $g.mol^{-1}$), poly(ethylene glycol) diacrylate (OEGDA, Mn = 250 $g.mol^{-1}$), methacrylic acid (MAA), potassium persulfate (KPS), potassium hydroxide (KOH, flakes), nitric acid (HNO_3, 52.5 %) were purchased from Sigma-Aldrich for the synthesis of bare and magnetic nanogels. Hepes hemisodium salt (dry powder)

and doxorubicin hydrochloride (DOX) were purchased from Sigma-Aldrich and used for *in vitro* and intracellular drug release studies. Acryloxyethyl thiocarbamoyl rhodamine B was purchased from Sigma-Aldrich. Human prostate cancer PC-3 cells (CRL-1435™) from ATCC®, Dulbecco's modified Eagle's medium (DMEM) from Sigma-Aldrich, foetal bovine serum (FBS) from Gibco, penicillin and Alamar Blue assay from Life Technologies were used for all the *in vitro* cell studies. All materials were used as received without any purification. Water was distilled and deionized.

2.2 Synthesis of pH- and Thermo-responsive NanoGels

Oligo(ethylene glycol) methacrylate based nanogels were prepared in a batch reactor by conventional precipitation radical co-polymerization in water and without using surfactants. Firstly, 50 mL distilled water were purged with nitrogen ($N_{2(g)}$) for at least 30 min at room temperature in order to remove oxygen. This purged water was used as solvent for the polymerization reaction. Then, MEO_2MA (0.62 g; 3.3 mmol) monomer; OEGMA (0.18 g; 0.36 mmol), MAA (0.019 g; 0.221 mol) co-monomers and OEGDA (0.035 g; 0.14 mmol) cross-linker were dissolved in 40 mL of distilled purged water and put into a round-bottom flask. This solution was heated at 70 °C, stirred at 400 rpm and purged with nitrogen for 1 h. For starting the polymerization reaction, KPS initiator solution (0.005 g, 0.0185 mmol dissolved in ^{10} mL of purged water) was introduced into the round-bottom flask. The solution became turbid after a few minutes. The polymerization reaction was allowed to continue under $N_{2(g)}$ at 70 °C, under reflux, with stirring for 5 h. Finally, the round-bottom flask was quickly immersed into an ice bath to stop the reaction. The final nanogels were then purified by dialysis against distilled water in order to remove unreacted reagents and impurities (using a Spectra / Por membrane, 12–14 kDa molecular weight cut off from Spectrum Laboratories). The water bath was changed for

fresh water two times a day until the conductivity of the water bath was close to that of distilled water (around 2 $\mu S.cm^{-1}$). In order to simplify writing, P(MEO_2MA-co-OEGMA-co-MAA) nanogels will be noted NanoGels thereafter.

2.3 Synthesis of Fluorescent RHO-NanoGels

In order to monitore doxorubicin (DOX) loaded nanogels internalization and DOX release inside cells by confocal fluorescent microscopy, we synthetized fluorescent rhodamine covalently bonded nanogels. In this case, a solution containing a rhodamine derivative co-monomer (acryloxyethyl thiocarbamoyl rhodamine B) was prepared (0.1 wt% relative to the other monomers, MEO_2MA / OEGMA / MAA). This solution was filtered through a porous membrane of 0.2 µm in order to remove any impurities and was introduced into the round-bottom synthesis flask. RHO-NanoGels were then synthetized following the procedure described above.

2.4 Synthesis of Magnetic Nanoparticles

Magnetic nanoparticles (MNPs) of maghemite (γ-Fe_2O_3) were synthetized by co-precipitation of metallic salts ($FeCl_2$ and $FeCl_3$) according to Massart's procedure[26]. A stable magnetic aqueous solution (ferrofluid, pH around 2), containing polydisperse, positively charged magnetic nanoparticles was obtained. Then, in order to reduce polydispersity, MNPs (with NO_3^- as counter ion) were sized-sorted, as stated by S. Lefebure et al.[27]. This procedure is based on the destabilization of positively charged MNPs dispersion by increasing the ionic strength of the medium. For this purpose, a concentrated nitric acid solution (HNO_3, 52.2 %) was added to the MNPs dispersion. When the destabilization was observed, the flocculate was separated from the supernatant by magnetic sedimentation and washed with acetone and ether. The precedent step

was repeated until having a phase with the desired size and dispersity. Only the ferrofluid fraction containing the biggest MNPs was used afterwards (TEM values: d = 11.5 nm and σ = 0.33; VSM values: d = 9.8 nm, σ = 0.28 and volume fraction ϕ = 1.98 %).

2.5 Encapsulation of Magnetic Nanoparticles into NanoGels

Magnetic nanogels, noted MagNanogels-X wt% (X = 9.0, 16.7, 28.6, 37.5, 50.0 and 66.7 wt% with X = $m_{MNPs} / \left[m_{MNPs} + m_{nanogels}\right]$) were prepared by loading preformed MNPs into thermoresponsive oligo(ethylene glycol) methacrylate based nanogels as described by Boularas et al.[28]. Briefly, for encapsulating the MNPs into nanogels, the pH of 5 mL of NanoGels solution ([nanogel] = 6.7 $g.L^{-1}$ determined by gravimetric measurements) was adjusted below 3.0 by addition of few drops of a nitric acid solution (0.1 M HNO_3). Then, a volume of MNPs solution depending on X (variable according to the desired concentration of MNPs), was added drop-by-drop to aqueous nanogels solution under stirring at room temperature. After 3 h, the pH was increased until 7.0 by addition of few drops of potassium hydroxide solution (0.1 M KOH); the solution was stirred overnight. Finally, MagNanoGels were washed several times by magnetic separation using a strong neodymium magnet (Nd-Fe-B, 1.22-1.26 T) and redispersed in water.

2.6 Encapsulation of Doxorubicin into MagNanoGels

The encapsulation of doxorubicin (DOX) into MagNanoGels was carried out by diffusion of molecules through the polymer matrix. Briefly, 1 mL of MagNanoGels at pH 7.5 (0.1 M sodium hepes buffer solution; [Fe] = 8.36 mM; [nanogels] = 2.94 $mg.mL^{-1}$) was mixed with 72 µL of DOX solution ([DOX] = 1 $mg.mL^{-1}$) and stirred during 24 h. After the encapsulation period, the excess of DOX (free DOX in solution and DOX adsorbed at the nanogels surface) was removed by several washing steps (10 min of magnetic separation). 1 mL of fresh hepes buffer solution

was then added on MagNanoGels and all supernatants were analyzed by UV-Vis spectrophotometry to deduce the DOX amount encapsulated and the loading efficiency (%) of magnetic nanogels.

$$DOX_{encapsulated} = initial\ amount\ of\ DOX - excess\ amount\ of\ DOX \quad \text{Eq. 1}$$

$$loading\ efficiency\ (\%) = \frac{DOX\ amount\ encapsulated}{initial\ amount\ of\ DOX} \times 100 \quad \text{Eq. 2}$$

2.7 *In vitro* Drug Release Triggered by Stimuli: Temperature, pH and Magnetic Hyperthermia

In vitro DOX release of MagNanoGels containing 37.5 wt% of MNPs was analyzed in different conditions to assess the influence of the pH, the temperature and the effect of an alternative magnetic field (AMF). We monitored DOX release in medium at pH 7.5 (0.1 M sodium hepes solution) and at pH 5.0 (0.05 M citric acid and 0.1 M sodium phosphate).

For magnetic hyperthermia drug release experiments: 1 mL of DOX-MagNanoGels solution ([Fe] = 0.5 mM; [nanogel] = 0.16 $mg.mL^{-1}$; [DOX] = 4.4 µM, loading efficiency = 63 %) in corresponding buffer solution (pH 7.5 or 5.0) was placed in an eppendorf inside the coil of the MagneTherm^{TM} system and AMF was applied by pulses of 30 min (335 kHz, 9 mT, 12.0 $kA.m^{-1}$). The temperature of the sample was monitored with a fluoroptic fiber thermometer and recorded every 1 s. After each AMF pulse, the supernatant was collected by magnetic separation (5 min). The amount of DOX release in each supernatant was quantified by UV-Vis spectroscopy. After the analysis, 1 mL of fresh buffer solution at the corresponding pH was added to magnetic nanogels. The same protocol was used for DOX release experiments without AMF, but in this case, the sample was placed in a water bath at the desired temperature (4, 25, 37, 50 and 70 °C).

2.8 Cell Culture

Human prostate cancer PC-3 cells (ATCC® CRL-1435™) were grown in adhesion in Dulbecco's modified Eagle's medium (DMEM) (Sigma-Aldrich) supplemented with 1 % penicillin and 10 % foetal bovine serum (FBS). They were kept at 37 °C in humidified atmosphere at 5 % CO_2 until confluence.

2.8.1 Incubation and Cell Labelling

PC-3 cancer cells were incubated at 37 ºC with an aqueous dispersion of MagNanoGels-37.5 wt%, a dispersion of DOX-MagNanoGels-37.5 wt% or with a DOX free solution ([Fe] = 0.13 to 4.1 mM in 5 %-citrated RPMI medium and [DOX] = 1.1 to 36.6 μM) for 2 hours. Control MNPs were incubated for the same period ([Fe] = 0.13 to 1.1 mM). After incubation, cells were washed twice with culture medium, and further incubated for 2 hours (chase period) in complete medium (DMEM supplemented with 10 % FBS) before treatments.

2.8.2 Quantification of the Cellular Uptake

The proportion of internalized MNPs in cells was determined by the amount of iron content per single cell through magnetophoresis. Briefly, after cells incubation with MNPs, MagNanoGels-37.5 wt% or DOX-MagNanoGels-37.5 wt%, cells were detached and suspended in a chamber subjected to a calibrated magnetic field gradient (gradB=145 $mT.m^{-1}$; B=17 $T.m^{-1}$) created by a permanent magnet. Single labeled cells migration towards the magnet was video-monitored and cell diameters (d_{cell}) and velocities (v_{cell}) were measured. The magnetization per cell (M_{cell}) was then computed for 200 independent cells by balancing the magnetic force (M_{cell}gradB) with the viscous drag ($3\pi\ \eta\ dc_{ell}v_{cell}$, η being the water viscosity). The mass of iron

per cell (m_{Fe}) is then proportional to M_{cell}. For the MNPs used here, a magnetic moment of 6.6 x 10^{-14} A.m² corresponds to 1 pg of iron.

2.8.3 Cytotoxicity Assay

Cell viability after application of different treatments (in presence of free DOX, MagNanoGels-37.5 wt% and DOX-MagNanoGels-37.5 wt% with and without AMF) was evaluated in the colorimetric Alamar Blue assay. Labelled and treated cells were incubated with 10 % Alamar Blue in DMEM for 2 hours. The Alamar Blue reagent was then transferred to a 96-well plate for analysis with a microplate reader (BMG FluoStar Galaxy) at an excitation wavelength of 550 nm with fluorescence detection at 590 nm. Viability was determined by comparison with control cells.

2.8.4 Intracellular Treatment under AMF

For AMF application, cells were first seeded in 1 cm diameter culture well and cultured until confluency. Then, after the incubation and chase period, the cells were submitted for 2 hours to an alternative magnetic field (AMF) produced by a generator device (NanoScale Biomagnetics) with a frequency of 470 kHz and an amplitude of 18 mT. Temperature was probed with a fluoroptic fiber thermometer and recorded every 1 s.

2.9 Characterization Techniques

2.9.1 Size Measurements

Dynamic Light Scattering (DLS): hydrodynamic diameter (d_h), polydispersity index (PDI) and zeta potential (ζ) of MNPs, NanoGels and MagNanoGels were measured with a Zetasizer

Nano ZS (Malvern Instruments) at 25 °C with an angle of 173 °. The measurements were repeated three times. For d_h measurements performed at different temperatures, the change of the water viscosity with temperature was taken into account. Samples were equilibrated for 10 min at each temperature before analysis. The diameter-temperature curves were carried out by heating (from 10 to 60 °C) and by cooling (from 60 to 10 °C), the d_h was measured every 2.5 °C. Each cycle was performed two times. The d_h of MagNanoGels before and after applying an alternative magnetic field (AMF pulse: 335 kHz, 9 mT, 12.0 $kA.m^{-1}$, 30 min) were also measured. All calculations (d_h and PDI) were performed using the Zetasizer software.

Transmission Electron Microscopy (TEM) and Cryo-TEM: size distribution parameters (diameter d, polydispersity σ) of MNPs, NanoGels and MagNanoGels were also characterized using a Jeol-100 CX TEM. A droplet of aqueous diluted nanogels dispersion was deposited on a carbon coated copper grid and dried at room temperature for at least 5 hours before TEM observations. Cryo-TEM images were taken with LaB6 JEOL JEM 2100 (JEOL, Japan) operating at 200 kV with a low dose system (Minimum Dose System, MDS). The samples were maintained at the desired temperature (25 and 50 °C) during one hour. Then, they were spread on a quantifoil holey-carbon-coated grid (Micro Tools GmbH, Germany) and quickly freezed by plunging the grid into liquid ethane. Images were recorded with an Ultrascan 2k CCD camera (Gatan, USA). Size distribution analysis were carried out on TEM and cryo-TEM images using ImageJ software and fitted to log-normal laws (standard error are based on n = 100 particles).

2.9.2 Gravimetric and Thermogravimetric Analysis (TGA)

The mass of nanogels per unit of volume of solution ($mg.mL^{-1}$) was evaluated by gravimetric measurement: 1 mL of nanogels solution was placed in a stove at 70 °C until all water was evaporated and the solid content was weighed afterward. Furthermore, MNPs content

encapsulated inside nanogels was determined by thermogravimetric analysis using a TGA SDT Q600, TA Instruments, using an aluminum melting-pot. Samples were analyzed under nitrogen with a flow rate of 100 mL $N_{2(g)}$.min^{-1} and at a heating rate of 10 °C.min^{-1} from room temperature 25 to 800 °C. The theoretical values of introduced MNPs were compared to the experimental fraction measured by thermogravimetric analysis (TGA).

2.9.3 Conductimetric and Potentiometric Analysis

The molar content of COOH per nanogel, the degree of ionization of –COOH functions (α) and their acidity constant (pKa) were calculated by conductimetric and potentiometric analysis as described by T. Hoare and R. Pelton[29]. Briefly, a freshly prepared solution of sodium hydroxide ([NaOH] = 6 mM) was used to titrate –COOH groups contained in 10 mL of NanoGels solution ([nanogel] = $1.0.10^{-3}$ g.mL^{-1}). In order to protonate all carboxylic acid groups, the pH of nanogels solution was previously adjusted below 2.5 by adding some drops of an HCl solution at 0.1 M. The molar content of COOH per nanogels (in mmol COOH.g^{-1} nanogels), α and the pKa were calculated as follows:

$$[COOH] = \frac{[NaOH]_{titrant} \times (V_{eq2} - V_{eq1})}{m_{nanogels}} \quad \text{Eq. 3}$$

$$\alpha_{(25°C)} = \frac{[COO^-Na^+]}{[COO^-Na^+]+[COOH]} = \frac{V_{NaOH} - V_{eq1}}{V_{eq2} - V_{eq1}} \quad \text{Eq. 4}$$

$$pKa = pH - log\left(\frac{\alpha_{(25°C)}}{1-\alpha_{(25°C)}}\right) = pK_0 + \frac{1}{\ln(10)} \cdot \frac{dG_{el}}{RTd\alpha} \quad \text{Eq. 5}$$

V_{eq1} and V_{eq2} are the volume of NaOH added to neutralize respectively the excess of HCl and the COOH groups. V_{NaOH} is the volume added for a given pH. pK_0 is the intrinsic dissociation constant independent of α, R is the gas constant, T is the absolute temperature and G_{el} is the electrostatic Gibbs energy term. The pK_0 can be estimated by extrapolating the α versus pH

curve back to $\alpha=0$[30]. Conductimetric and potentiometric curves are provided in the supporting information report (Figure S1 – S2). The conductivity titration curve has three distinct zones: zone I corresponds to the neutralization of excess H^+ (from HCl) by OH^- ions (from NaOH). In zone II, the deprotonation of carboxylic acid groups by OH^- ions is observed and in zone III, there is an excess of OH^- ions, raising the conductivity of the solution.

2.9.4 Iron Titration

The total iron concentration [Fe] was determined by atomic absorption spectroscopy using a Perkin-Elmer Analyst 100 system after completely degradation of MNPs with 10 times their volume in HCl (35 %).

2.9.5 Magnetic Measurements

Vibrating Sample Magnetometer (VSM): magnetic properties of MNPs were measured using a VSM. A diluted aqueous solution of MNPs was prepared (volume fraction of nanoparticles $\phi < 2\%$). The magnetization curve M(H) of a suspension of monodisperse iron oxide nanoparticles can be described by a Langevin's law[31]. Assuming a log-normal distribution P(d) and fitting the theorical to the experimental magnetization curve, we can calculate the magnetic diameter (d_0) and the polydispersity index (σ) of MNPs solutions.

Superconducting Quantum Interference Device (SQUID): the magnetic properties of MNPs and MagNanoGels were studied using a SQUID magnetometer. Samples were analyzed at 298 K by increasing the magnetic field from zero to 50 kOe; decreasing it to -50 kOe and finally increasing it back to zero.

Magnetic Hyperthermia Experiments: The specific loss power (SLP) of MNPs and the drug release kinetics of DOX-MagNanoGels-37.5 wt% were carried out with a MagneTherm™

system (Nanotherics, UK) equipped with a fluoroptic fiber thermometer. The sample was heated at 23 or at 37 °C before the application of an alternative magnetic field (335 kHz, 9 mT, 12.0 $kA.m^{-1}$, 30 min). For studies at a higher frequency and higher magnetic field (470 kHz, 18 mT) and for cell studies, an alternating magnetic generator device (NanoScale Biomagnetics) was used.

2.9.6 UV-Visible Spectrophotometry

DOX encapsulation and release were monitored by absorbance measurements using an Avantes UV-visible spectrophotometer (100 μm optical fiber; deuterium-halogen light source) with wavelengths from 200 to 800 nm. Two calibration curves of DOX were performed from the UV absorbance at λ_{max} = 485 nm in two different buffer solutions: at pH 7.5 (0.1 M sodium hepes) and at pH 5.0 (0.05 M citric acid; 0.1 M sodium phosphate). Molar absorption coefficients are $\varepsilon_{pH7.5}$: 13.1 $mL.mg^{-1}.cm^{-1}$ and $\varepsilon_{pH5.0}$: 11.6 $mL.mg^{-1}.cm^{-1}$ respectively.

2.9.7 Confocal Imaging

Fluorescent RHO-MagNanoGels were synthesized by covalently grafting with rhodamine B (RHO; $\lambda_{Ex.}$= 548 nm; $\lambda_{Em.}$ = 570 nm). The internalization of RHO-MagNanoGels, DOX loaded RHO-MagNanoGels and free DOX inside PC-3 cancer cells was analyzed by confocal microscopy. Cells were observed with an Olympus JX81/ BX61 Device/Yokogawa CSU Device spinning disk microscope (Andor Technology plc, Belfast, Northern Ireland), equipped with a 60x Plan-Apon oil objective lens. The rhodamine B was excited with laser at 561 nm, and fluorescence emission collected in the red channel at 604 nm. Doxorubicin (DOX) was excited with laser at 488 nm, and fluorescence emission collected in the green channel at 561 nm. To quantify the amount of nuclear DOX, a measurement of the cell nucleus was carried out by

drawing circular areas included in the nucleus shape and measuring the average fluorescence intensity within (n > 10 cells). The intensity of the fluorescence is correlated with the amount of DOX internalized in the nucleus. Intracellular DOX release under AMF experiments were also monitored by confocal microscopy.

3. RESULTS AND DISCUSSION

3.1 Synthesis and Characterization of NanoGels

Nanogels based on oligo(ethylene glycol) methacrylate (macro)-monomers (MEO_2MA; OEGMA), functionalized with methacrylic acid (MAA) were synthetized by aqueous precipitation radical co-polymerization. The number of carboxylic functions (-COOH) per nanogel was deduced from conductimetric and potentiometric titrations of methacrylic acid functions inside nanogels (Figure S1). According to the equation 3 (experimental section), there are 0.38 mmol of COOH per gram of NanoGels. The pH (Eq. 4 and Eq. 5) as a function of the degree of ionization (α) of MAA units at 25 °C was calculated and plotted (Figure S2). The intrinsic dissociation constant of NanoGels (pK_0) was estimated by extrapolating the α versus pH curve back to α=0.[30, 32] This value (pK_0=4.5) is close to the pK_0 of linear poly(methacrylic acid) (pK_0=4.65). Similar results were obtained by M. Boularas et al.[33] for nanogels based on the same monomers (MEO_2MA, OEGMA and MAA).

NanoGels exhibit well-defined and spherical morphology in TEM images (Figure S3), have an average hydrodynamic diameter (d_h) of 328 nm at 25 °C, are highly monodispersed and are negatively charged in distillated water (pH 5.5), showing a zeta potential of -35.4 mV. As shown in Figure 1a, these nanogels present a swelling-deswelling behavior when the temperature is increased. Indeed, the d_h decreases from 354 nm (at 10 °C) to 272 nm (at 60 °C) at pH 5.5; and from 650 nm (at 10 °C) to 422 nm (at 60 °C) at pH 7.5 (Figure 1a). Experimental d_h versus temperature curves were fitted by a nonlinear regression estimated by least square method, in order to assess the inflection point of fitted curves, corresponding to the volume phase-transition

temperature (VPTT). The VPTT of NanoGels is 30 °C at pH 5.5 and 54 °C at pH 7.5. Below the VPTT, the nanogels aqueous solution is limpid, while for T > VPTT a higher turbidity is observed. Indeed, below the VPTT, the polymer and water molecules form hydrogen bonds, leading to swelling of the nanogels. However, with increasing temperature at T > VPTT, the hydrogen bonds are destroyed and hydrophobic interactions of the polymer appear, collapsing nanogels' matrix and expelling the water.

Due to the presence of carboxylic groups (–COOH) from methacrylic acid co-monomer, NanoGels are pH-responsive. Figure 1b shows the corresponding pH-dependence of the hydrodynamic diameter of NanoGels. Their d_h increases when the pH increases, from 315 nm at pH 2.0 to 545 nm at pH 9.0. When the pH < 6.5, the (–COOH) groups are mostly undissociated, thus nanogels are weakly negatively charged and behave like uncharged particles. In that case, the d_h of nanogels is only determined by the temperature. On the contrary, when pH > 6.5 the (–COOH) groups start dissociating and forming carboxylate groups ($–COO^-$), therefore nanogels are charged and fully swollen due to electrostatic repulsions between polymer chains. Here, the swelling of the nanogels is dominated by ionic contributions, mainly strong electrostatic repulsions between close ionic groups.

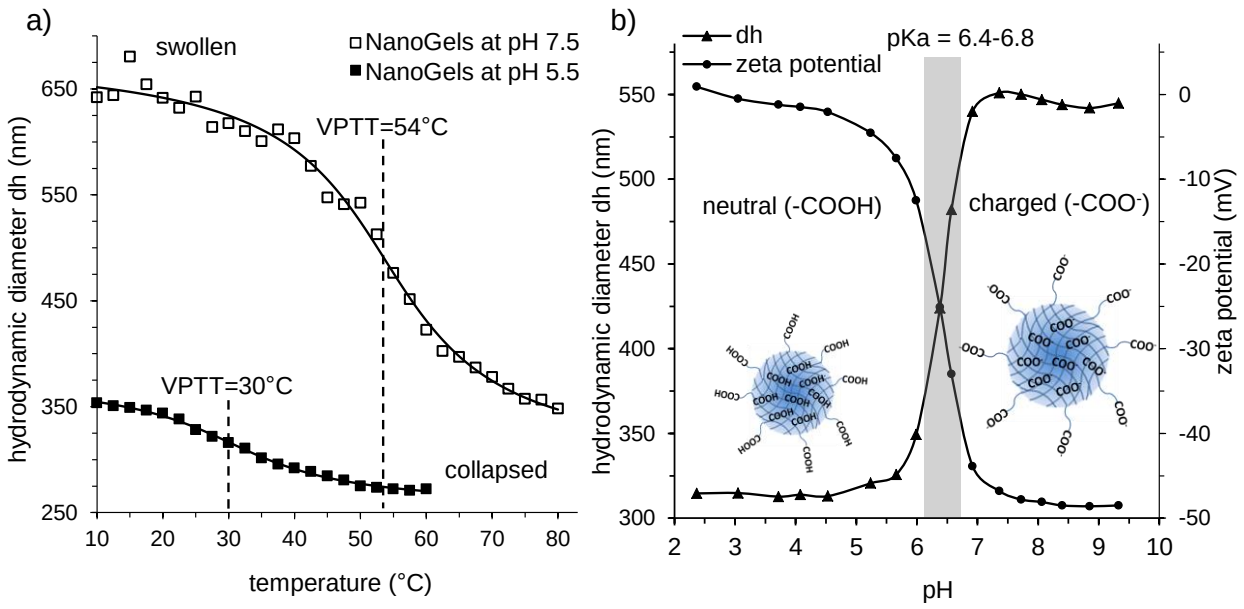

Figure 1. a) The hydrodynamic diameter (d_h) as a function of the temperature and b) the d_h and the zeta potential (ζ) of NanoGels as a function of the pH measured by DLS.

3.2 Synthesis and Characterization of MagNanoGels

To synthesize MagNanoGels, we adopted a similar strategy to the one employed by M. Boularas et al.[28] Some parameters were modified, like the reaction time and the purification method. This method, based on the assembly of preformed MNPs inside nanogels by complexation of carboxylic acid groups of the polymer matrix onto the surface of magnetic nanoparticles, provides monodisperse nanogels with high content of homogeneously distributed magnetic nanoparticles and ensures good properties of the two colloidal systems, the nanogels and the MNPs.

The iron oxide nanoparticles (γ-Fe_2O_3) were synthetized by co-precipitation of metallic salts $FeCl_2$ and $FeCl_3$ according to Massart's process[26]. They have a "rock-like" shape, as observed in TEM images (Figure S4). They are positively charged (ζ = 25.3 mV) and are stabilized by electrostatic repulsions in acidic medium. It has been demonstrated that their heating power can

be improved by increasing particles diameters and reducing polydispersity[34]. Therefore, the MNPs were size-sorted and only the fraction containing the larger particles was used to prepare MagNanoGels (d = 11.5 nm and σ = 0.33 obtained by TEM). The MNPs were incorporated into nanogels by changing gradually the pH of the solution from 3.0 to 7.0. At pH 3.0, the MNPs are positively charged and the nanogels are neutral; thus the MNPs can diffuse easily through the polymer matrix without flocculation. At pH 7.0, the MNPs bear no charge and carboxylate groups can bound to the surface of MNPs by a complexation reaction[35]. Magnetic nanoparticles were incorporated into nanogels at various mass ratio (X = 9.0, 16.7, 28.6, 37.5, 50.0 and 66.7 wt%; with $X = m_{MNPs} / [m_{MNPs} + m_{nanogels}]$). Magnetic nanogels with X > 50.0 wt% could not be measured by DLS because of their instability. In distilled water (pH 5.5) at 25 °C (swollen state), the d_h of MagNanoGels increases as the MNPs mass ratio increases, from 342 nm to 460 nm for nanogels containing 9.0 to 37.5 wt% of MNPs respectively (Table 1). At 50 °C (collapsed state), the d_h of nanogels containing MNPs is bigger than the d_h of bare nanogels (295 nm vs. 275 nm for magnetic and non-magnetic nanogels respectively), but it no longer depends on the MNPs mass ratio and remains around 300 nm. All nanogels are weakly negatively charged in distilled water (pH 5.5), because of some deprotonated carboxylic acid groups. The more MNPs are added, the more the charge of nanogels increases, from -35.4 to -24.7 mV for NanoGels and MagNanoGels-37.5 wt% respectively. Carboxylic acid groups are essential for the structure and physicochemical properties of the magnetic nanogels. It allows: (1) to load magnetic nanoparticles into nanogels by complexation of iron atoms onto the surface of the MNPs, (2) to increase the VPTT value of the oligo (ethylene glycol) copolymers in order to have a temperature up to 37 °C in physiological conditions by increasing the hydrophilicity of nanogels,

(3) to have pH-sensitive nanogels and (4) to encapsulate a drug by electrostatic or hydrogen bonding interactions.

The swelling ratio (Q) of nanogels was calculated using the following equation:

$$Q = \frac{V_{swollen\ nanogels}}{V_{deswollen\ nanogels}} = \frac{V_{dh\ at\ 25\ °C}}{V_{dh\ at\ 50\ °C}} \quad \text{Eq. 6}$$

Q depends on the degree of crosslinking of polymer matrix and is directly related to the quantity of water that it can be loaded and released by nanogels. The swelling ratio remains the same for non-magnetic nanogels at pH 5.5 and pH 7.5 (Q = 1.7), but it decreases from Q = 3.7 to 1.6 for MagNanoGels-37.5 wt% when the pH increases from 5.5 to 7.5. All the parameters of magnetic nanogels containing various MNPs mass ratios are given in the Table 1.

Table 1. Characteristics of MagNanoGels-X wt% loaded with various MNPs mass ratio (from X = 0 to 37.5 wt%) at pH 5.5 and 7.5 *

pH	**5.5**					**7.5**	
X (wt%)	0	9.0	16.7	28.6	37.5	0	37.5
d_h at 25°C (nm) (PDI)	328 (0.021)	342 (0.086)	337 (0.107)	374 (0.132)	460 (0.364)	643 (0.087)	584 (0.371)
d_h at 50°C (nm) (PDI)	275 (0.037)	295 (0.039)	295 (0.047)	310 (0.115)	298 (0.312)	542 (0.078)	495 (0.367)
Q	1.70	1.56	1.50	1.76	3.68	1.66	1.64
ζ (mv)	-35.43	-32.63	-29.80	-29.35	-24.67	-12.67	-10.62
VPTT (°C)	30.31	25.95	21.75	24.91	28.57	53.54	47.01

* The hydrodynamic diameter (d_h) and PDI at 25 and 50 °C; the swelling ratio (Q), the zeta-potential (ζ) and the Volume Phase Temperature Transition (VPTT) were measured by DLS.

Furthermore, as we can observe by TEM, MNPs seem to be homogeneously distributed (no aggregates) in nanogels, when the MNPs mass ratio is below 50 wt% (Figure 2a to d). However, this is a 2D projection, so it is difficult to localize the MNPs in the structure (shell versus core for

example). The "honeycomb" structure is due to the drying of nanogels on the TEM grid. For higher content in MNPs (X > 50 w%), some aggregates appear on the surface of the nanogels (Figure 2e) and for X = 66.7 wt%, nanogels look like capsules with a more dense shell (Figure 2f).

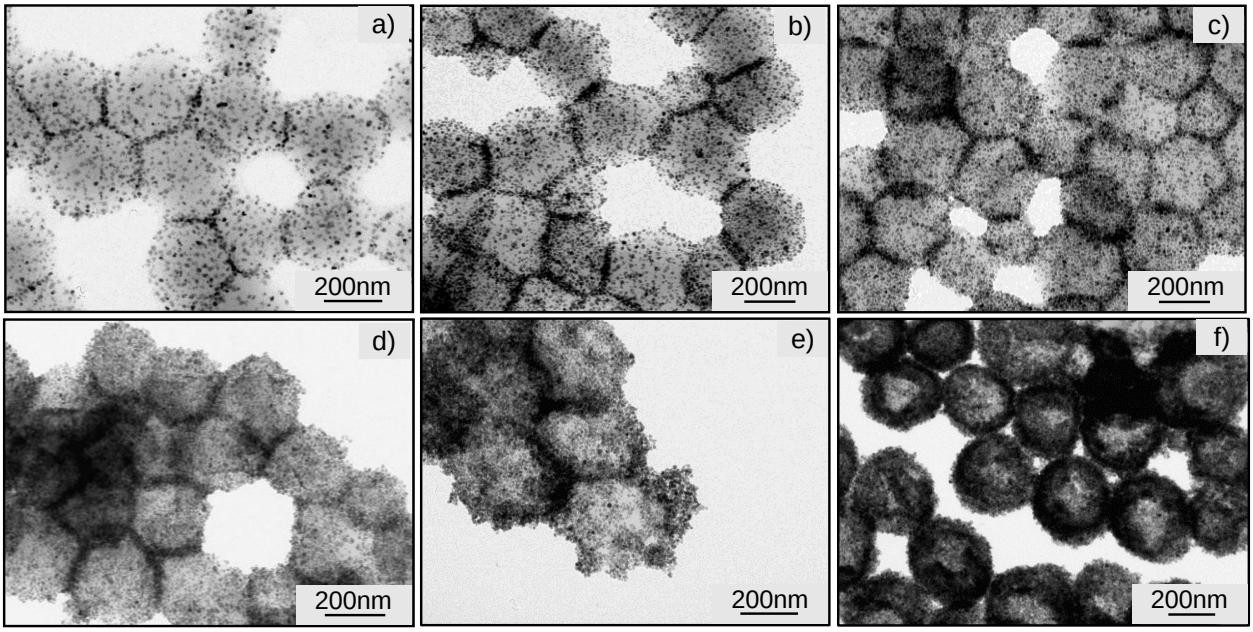

Figure 2. TEM images of MagNanoGels-X wt% loaded with X = 9.0, 16.7, 28.6, 37.5, 50.0 and 66.7 wt% of MNPs (from a to f respectively). MNPs are homogeneously distributed inside nanogels. When X > 50 wt% (e, f) nanogels are not stable in water.

The incorporation of MNPs into nanogels can be quantified by TGA as shown from the TGA curves of MNPs, NanoGels and MagNanoGels (Figure S5). As expected, the mass of NanoGels decreases sharply from 225 to 430 °C due to the thermal decomposition of polymer matrix. The TGA curve shows a total weight loss above 450 °C. When incorporating MNPs, the weight loss decreases from 87 to 70 % depending on the MNPs loading percent. These results confirm the effective presence of MNPs in the MagNanoGels.

3.3 Thermo- and pH-sensitivity of NanoGels and MagNanoGels

MagNanoGels are multi-stimuli responsive nanocarriers, sensitive to pH (via carboxylic acid groups), temperature (via oligo(ethylene glycol) monomers) and magnetic fields (via MNPs).

The evolution of the d_h at different temperatures of MagNanoGels-X wt%, loaded with different MNPs content (MNPs mass ratio X = 9.0, 16.7, 28.6 and 37.5 wt%), was analyzed by DLS. These measurements reveal that the d_h of all magnetic nanogels decreases while temperature increases, proving their thermoresponsive swelling-deswelling behavior (Figure 3a). So for example, d_h decreases from 460 nm at 25 °C to 298 nm at 50 °C for magnetic nanogels containing 37.5 wt% of MNPs (Δd = 30 nm). This swelling-deswelling behavior is fully reversible and seems to be independent of the amount of MNPs contained into nanogels, at pH 5.0 the VPTT of all magnetic nanogels remains around 25 °C.

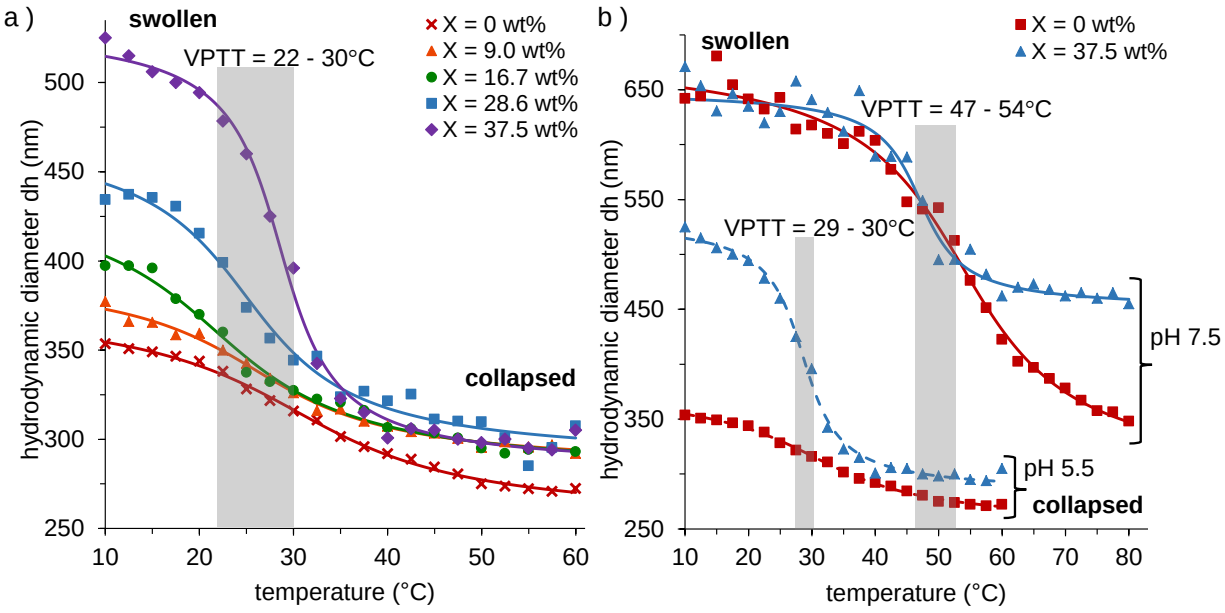

Figure 3. a) Diameter-temperature curves of MagNanoGels-X wt% in water (pH 5.5) and b) at different pH: in water (pH 5.5) and in a physiological medium (0.1 M hepes buffer saline solution, pH 7.5) measured by DLS.

The charge density of nanogels, which depends on the pH of the medium, also modifies their temperature-dependent swelling behavior with a shift of the VPTT towards higher temperatures when increasing the pH. Thus, the VPTT of MagNanoGels-37.5 wt% rises from 28.6 to 47.0 °C, when changing the pH from 5.5 to 7.5 (Figure 3b). Since the VPTT of the nanogels is higher than 37 °C (human body temperature) under physiological conditions (pH 7.5), these nanogels could be used as "on-demand" drug release nanocarriers for biomedical applications.

3.4 Magnetic Properties of MNPs and MagNanoGels

The magnetization versus applied magnetic field curves, obtained by SQUID measurements, confirm the superparamagnetic properties of MNPs and MagNanoGels (Figure 4a). Indeed, they have zero coercitivity and remanence (inset of Figure 4a). The saturation magnetization (Ms) value of MNPs and MagNanoGels-37.5 wt%, containing the same iron concentration ([Fe] = 11.5 mM), are respectively 98 and 96 $emu.g^{-1}$ at 50 kOe. Thus, the Ms of MNPs remains the same after their incorporation into nanogels.

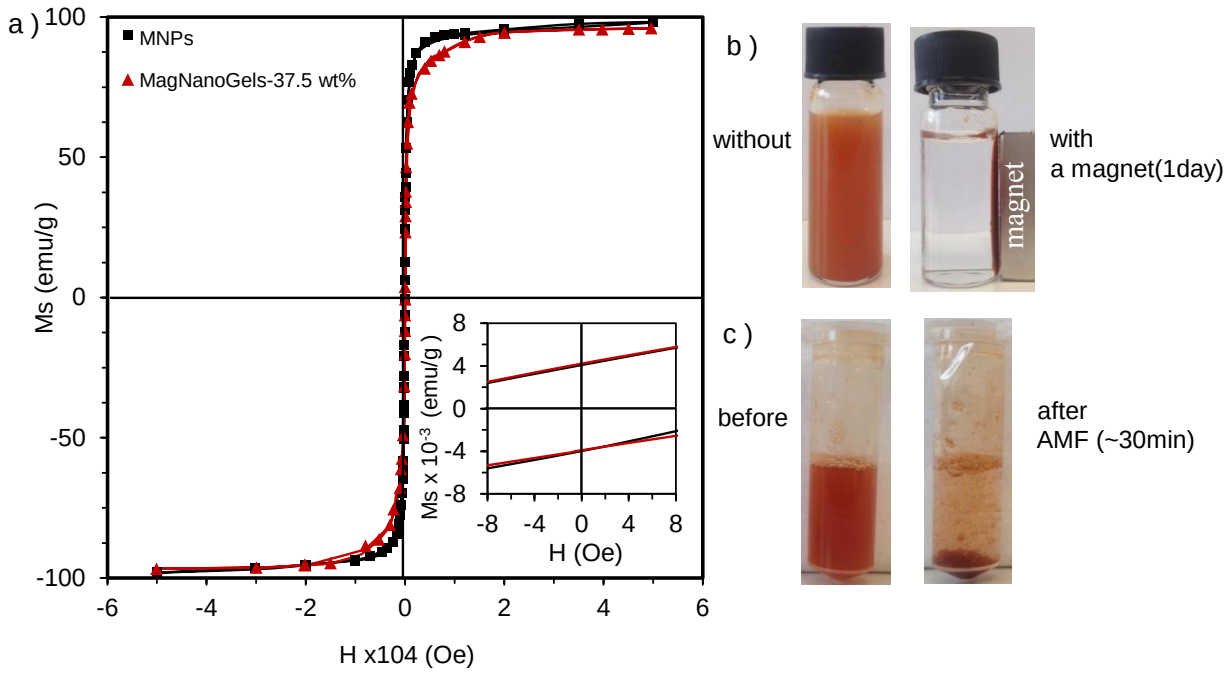

Figure 4. a) Magnetization curve of MNPs and MagNanoGels-37.5wt% at 298 K, measured by SQUID and magnetic behavior of these nanogels in the presence of b) a permanent magnet (Nd-Fe-B, 1.22-1.26 T) and c) an alternative magnetic field AMF (335 kHz, 9 mT, 12.0 $kA.m^{-1}$).

MagNanoGels are well dispersed in water if neither permanent nor alternative magnetic fields are applied. As shown in Figure 4b, nanogels can be collected using a permanent magnet. In response to the permanent magnetic field, nanogels move and form a pellet on the container wall near the magnet. This technique was used for the purification of magnetic nanogels after their synthesis. Otherwise, nanogels aggregate under an alternative magnetic field (AMF), but this aggregation is reversible (Figure 4c).

Furthermore, superparamagnetic nanoparticles generate heat under an alternative magnetic field (AMF).[34] This phenomenon is called "magnetic hyperthermia". Heat dissipation is governed by Néel (rotation of the magnetic moment) and / or Brown (rotation of the particles) relaxations. It was demonstrated that, for maghemite nanoparticles produced by coprecipitation of iron salts such as the ones used here, with diameter below 16 nm, the heat dissipation is

mainly controlled by Néel relaxation[34]. In order to assess the efficacy of MNPs as magnetic hyperthermia source, the specific loss power (SLP, in $W.g^{-1}$ of MNPs or in $W.g^{-1}$ of iron) of MNPs and MagNanoGels-37.5 wt% were calculated according to the equation below:

$$SLP = \frac{C_p}{\rho \cdot \phi} \cdot \left[\frac{d\theta}{dt}\right]_T \quad \text{Eq. 7}$$

where C_p is the specific mass heat capacity of the solvent ($C_{p\,water}$ = 4.184 $J.K^{-1}.g^{-1}$), ρ is the density of magnetic nanoparticles ($\rho_{MNPs} = 4.9$) and ϕ is the volume fraction of MNPs in the ferrofluid or inside the nanogels. The evolution of the temperature was monitored in situ using a non-metallic fluoroptic fiber thermometer when applying AMF (335 kHz, 9 mT, 12.0 $kA.m^{-1}$) during 2 min at 25 °C. At 335 kHz, the SLP of MNPs and MagNanoGels-37.5 wt% are similar (SLP_{MNPs}=47 $W.g^{-1}$ Fe and $SLP_{nanogels}$=55 $W.g^{-1}$ Fe), therefore the MNPs preserve their heating power after being loaded into nanogels.

Moreover, as shown in Figure S6 a, the temperature of a highly concentrated MNPs solution ([Fe] = 1.14 M, ϕ = 1.8 %;) increases drastically from 20 to 46 °C (**Δ**T = 26 °C) after being exposed to AMF (335 kHz, 9 mT, 12.0 $kA.m^{-1}$, 2 min). For a 10-fold less concentrated solution, the temperature increases from 20 to 24 °C (ΔT = 4 °C); and for a sample diluted 100 fold, the temperature remains nearly constant (20 °C). The same behavior is observed for MagNanoGels solutions (Figure S6 b). Hereafter, the MagNanoGels solutions were used very diluted in order to avoid global heating and to study the possibility of remotely controlled the swelling-deswelling transition of magnetic nanogels under AMF in athermal conditions.

For this purpose, the evolution of the hydrodynamic diameter of MagNanoGel-37.5 wt% ([nanogels] = 2.9 $mg.mL^{-1}$; ([Fe] = 8.4 mM), before and after applying AMF, were monitored by DLS. As expected, the global temperature of these MagNanoGel-37.5 wt% diluted solutions did not increase (athermal conditions). Otherwise, the d_h decreases from 301 to 273 nm (Δd_h = 28

nm) when applying AMF during 30 min. These results were confirmed by cryo-TEM observations. As shown in Figure 5a, before applying AMF, magnetic nanoparticles are uniformly distributed into polymer matrix and mainly between the polymeric chains of nanogel brush. After applying AMF, the average diameter of MagNanoGels decreases from 462 to 430 nm (Δd = 32 nm) and the MNPs became closer to the surface of nanogels forming a "corona", in accordance to the swelling-deswelling behavior of polymer chains (Figure 5b). Indeed, before AMF, T < VPTT and polymer chains are hydrophilic and well swollen in the solution.

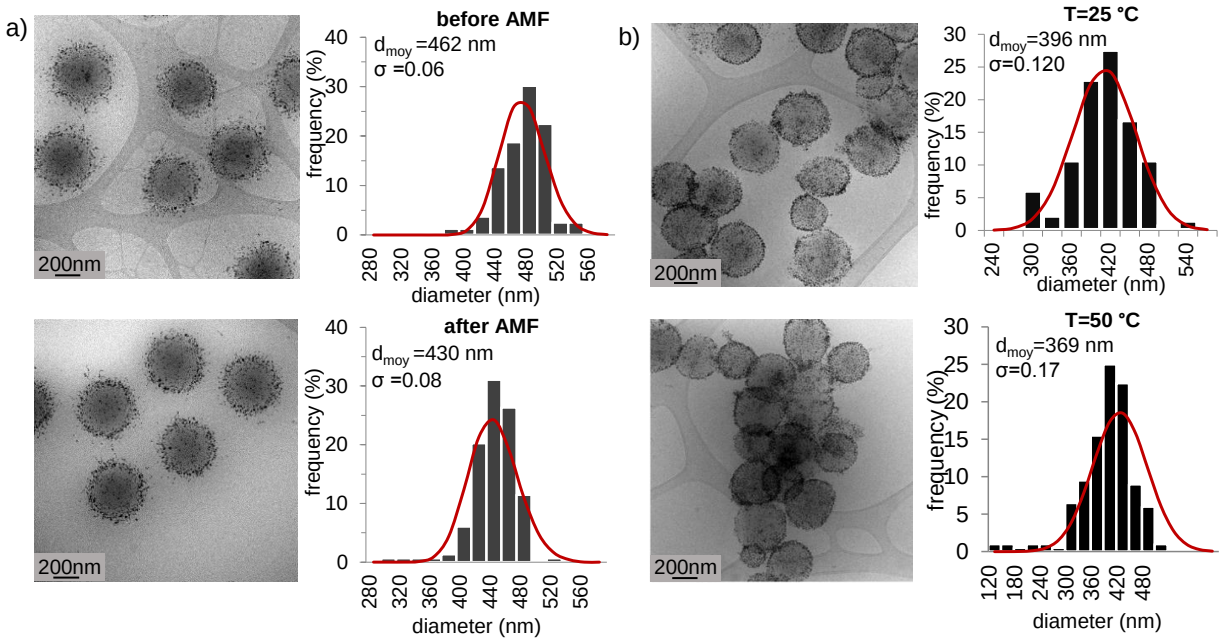

Figure 5. Evolution of the diameter of MagNanoGels-37.5 wt% a) by applying AMF at 335 kHz, 17 mT, 30 min (localized magnetic heating) and b) by placing the sample in an oven at 50 °C (macroscopic heating) and monitored by cryo-TEM (Δd ≈ 30 nm). Standard error based on n = 80 particles.

These results suggest that under AMF and in athermal conditions, the polymer chains become hydrophobic and collapse, decreasing the polymer chains length and reducing the interparticles distance. This prove that under AMF, the MNPs inside nanogels act as "hot spots" and only generate a local heating at nanometric scale, and that this heat is sufficient to cause the

deswelling of nanogels. For the MagNanoGels having the highest mass ratio of MNPs (66.7 wt%), the reduction of diameter is lower ($\Delta d \approx 15$ nm). These nanogels not only look like capsules with a more dense shell, but they also have a more rigid structure because of their high load in magnetic nanoparticles, which limits their deswelling (Figure S8).

Furthermore, it is interesting to compare cryo-TEM images wherein the temperature of magnetic nanogels was increased by placing the sample in an oven (macroscopic heating) and by applying AMF (localized magnetic heating) (Figure 5). Comparing different cryo-TEM images, it was noted that after macroscopic heating, MagNanoGels were more or less deformed, and that some of them shrank much more than others. On the contrary, after localized magnetic heating, nanogels shrank but kept their spherical shape. This can be explained by different heat diffusion mechanisms. During macroscopic heating, the heat diffuses from the outside to the inside of nanogels matrix, whereas during magnetic heating, each MNP acts as a "hot spot" and the heat is distributed homogeneously throughout the polymer matrix, assuming that the MNPs are distributed inside the nanogels.

3.5 Drug Release from DOX-loaded, pH- and Thermo-responsive MagNanoGels

MagNanoGels can be used as drug delivery systems (DDS) given that their polymer matrix is able to uptake and release high quantities of drugs. Moreover, we have shown above that the swelling-deswelling transition of MagNanoGels can be triggered by various stimuli: temperature, pH and magnetic field. Therefore, the responses to these three stimuli for *in vitro* and intracellular remotely controlled release of drug were investigated.

3.5.1 Encapsulation of DOX into MagNanoGels

Doxorubicin (DOX) is one of the most commonly used drugs to treat several types of cancer. However, it is well known that free DOX could have adverse effects on human body, such as cardiotoxicity and nephrotoxicity and that the encapsulation of the drug in polymeric nanocarriers (polymersomes, dendrimers, molecularly imprinted polymers, nanogels) may be a way to reduce side effects[36,37]. The encapsulation of DOX into MagNanoGels-37.5 wt% was carried out by diffusion of molecules through the polymer matrix at pH 7.5 (0.1 M sodium hepes buffer) and room temperature. Then the excess of drug was removed by repeated washing and magnetic separation steps, until there is no more drug left in the supernatant. The chemical stability of DOX in buffer's solutions has already been studied elsewhere[38]. The best storage conditions for long-time DOX stability are acidic medium (pH < 4) and low temperature (4 – 6 °C), thus DOX hepes buffer solution was freshly prepared before each encapsulation experiment. After having analyzed all the supernatants by UV-Vis spectrophotometer, the amount of DOX encapsulated and the loading efficiency (%) of MagNanoGels were calculated using a calibration curve (Figure S9) and equations 1 and 2 (experimental section). All encapsulation experiments were carried out using 1 mL of hepes solution containing 2.94 $mg.mL^{-1}$ of MagNanoGels-37.5 wt% and 115.8 µM of DOX. In these conditions, nanogels could be loaded with 69.5 µM of DOX, which corresponds to 63 % of loading efficiency (average of 10 experiments).

3.5.2 DOX Release Triggered by Temperature

The release profiles of DOX from DOX-MagNanoGels-37.5 wt% at pH 7.5 have been studied at various temperatures (4, 23, 37, 50 and 70 °C) in order to show the thermosensitivity of magnetic nanogels for triggered drug release. To reach the desired temperature, the samples were placed in a water bath. Each release experiment was carried out in triplicate, and average values were calculated and used to plot cumulative DOX release profiles. As shown in Figure 6, the

cumulative DOX release increases when the global temperature rises. After 4 h, MagNanoGels release 17 % (11.8 µM), 24 % (16.7 µM), 32 % (22.2 µM) and 36 % (25.0 µM) at respectively 23, 37, 50 and 70 °C. The release profile of DOX at 37 °C and pH 7.5 (yellow curve) was carried out in order to be placed in the same conditions of *in vitro* upcoming cancer cells studies. Furthermore, DOX-MagNanoGels can be well stored at low temperature; in fact DOX release was negligible when DOX-MagNanoGels solutions were stored at 4 °C (blue curve). After 1 month at 4 °C, less than 20 % (13.9 µM) of DOX was released.

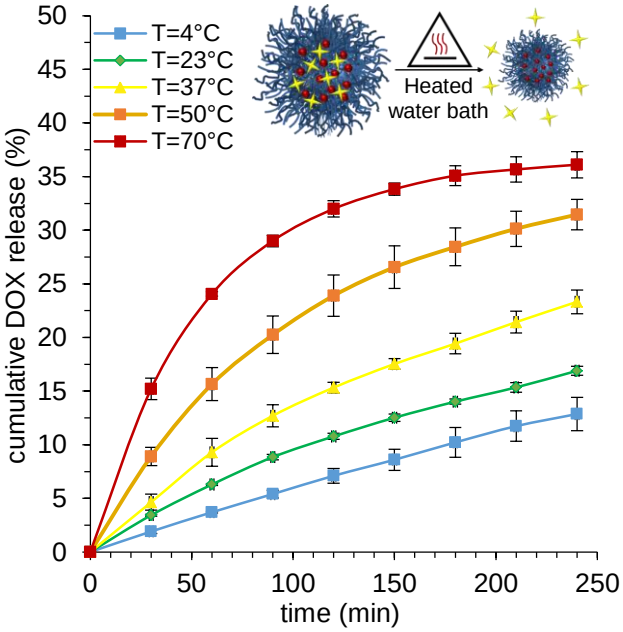

Figure 6: Cumulative DOX release profile (%) versus time of DOX-MagNanoGels-37.5 wt% ([Fe] = 8.4 mM) in buffer solution (pH 7.5, 0.1 M sodium hepes) at different temperatures. DOX release was calculated from UV-vis absorbance measurements, tracking the absorbance at 485 nm. Standard error based on n = 3 samples.

3.5.3 DOX Release Triggered by pH and Alternative Magnetic Field

We investigated the potential application of these magnetic nanogels for remotely controlled drug delivery by variations of the pH (internal stimuli) and by applying an alternative magnetic field (external stimuli).

After 4 h, at 37 °C and pH 7.5, only 24 % (16.7 µM) of DOX was released whereas at pH 5.0, the release of drug highly increased and reached 96 % (66.7 µM) (Figure 7). This pH-responsive behavior of MagNanoGels is very important for further cancer treatment, because DOX release can be limited in a normal physiological environment (pH 7.5). And, after cancer cell internalization, DOX release can be accelerated due to the acidic intracellular environments (lysosomes at pH 4.5). This pH-sensitivity can be explained by electrostatic interactions between DOX and MagNanoGels. At pH 7.5, DOX release is restricted by interactions between negatively charged nanogels (COO^-) and positively charged amino group (NH_3^+) of DOX. At pH 5.0, the carboxyl groups of MagNanoGels are mostly protonated (COOH), thus reducing interactions with the drug, but also reducing the d_h of nanogels, so expelling more drug. These results are in good agreement with recently reported results of pH-sensitive nanogels functionalized with carboxylic acid groups (from acrylic acid co-monomer)[6,39].

Otherwise, when applying an alternative magnetic field by pulses (335 kHz, 9 mT, 12.0 $kA.m^{-1}$, 30 min) DOX release was significantly enhanced at both pH conditions: after 4h at pH 7.5, MagNanoGels released two-fold more drug under AMF (47 % – 32.7 µM vs. 24 % – 16.7 µM); and at pH 5.0 all the DOX was expelled out of the MagNanoGels under AMF (100 % – 69.5 µM vs. 96 % – 66.7 µM) (Figure 7). If a higher AMF is applied (470 kHz; 18 mT; 14.4 $kA.m^{-1}$), DOX release slightly increases compared to a DOX release with AMF at 335 kHz (Figure S10). These results demonstrate that MagNanoGels can be used for remotely trigger of DOX under

AMF and that localized heating generated by MNPs is sufficient to highly increase drug delivery without macroscopic heating.

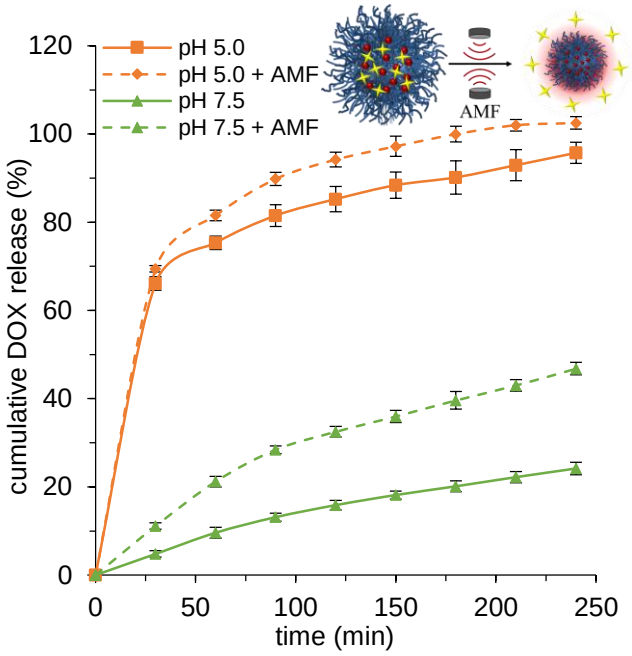

Figure 7. Cumulative DOX release profile (%) versus time of DOX loaded MagNanoGels-37.5 wt% ([Fe] = 8.35 mM) in physiological (pH 7.5; 0.1 M hepes sodium) and acidic (pH 5.0; 0.05 M citric acid and 0.1 M sodium phosphate) conditions at 37 °C without and with AMF (each AMF pulse: 335 kHz, 9 mT, 12.0 $kA.m^{-1}$, 30 min). DOX release was calculated from UV-vis absorbance measurements at 485 nm. Standard error is based on n = 3 samples.

During AMF experiments, the temperature of the sample was monitored with a non-metallic fluoroptic fiber thermometer and no macroscopic heating was detected (because of the low MNPs concentration). However, we have demonstrated that the d_h of MagNanoGels decreases under AMF due to a local heating of MNPs, not measurable by conventional thermometers. Thus, the heat generated under AMF is enough to provoke a shrinking of polymer network and enhances DOX release. This “hot spot” or “local magnetic hyperthermia” effect has already been observed for other DDS based on polymers (e.g. MNPs coated with polymers[13,18]; MIP-

nanoparticle[16]; polymersomes[40]). Concerning nanogels, the most studied systems for remotely drug delivery by applying AMF are based on poly(N-isopropylacrylamide) (PNIPAM)[9,41]. However, after purification the PNIPAM matrix may still contain some monomer of NIPAM, which is highly cytotoxic[42,43]. Additionally, PNIPAM may also interact with proteins because of the presence of several amide functions in its chemical structure[44]. For these raisons, it is very difficult to use them for biomedical applications, contrary to MagNanoGels based on biocompatible, water soluble, non-toxic poly(ethylene glycol) analogues[45].

Otherwise, quantifying the local temperature generated by MNPs under AMF is very important for biomedical applications. Some authors have used fluorophores as molecular thermometers for estimating the temperature at the nanometer scale[17,46]. In our case, data from Figure 6 were used to plot the release of DOX in function of the temperature at pH 7.5 and at different times (Figure 8a). These curves were used as calibration curves for acquire a quantitative correlation between DOX release and the local temperature under AMF. When applying one or more AMF pulses, the global temperature of MagNanoGels solutions remains as initially set (37 °C) and the local temperature was estimated around 65 °C (ΔT = 28 °C – Figure 8b).

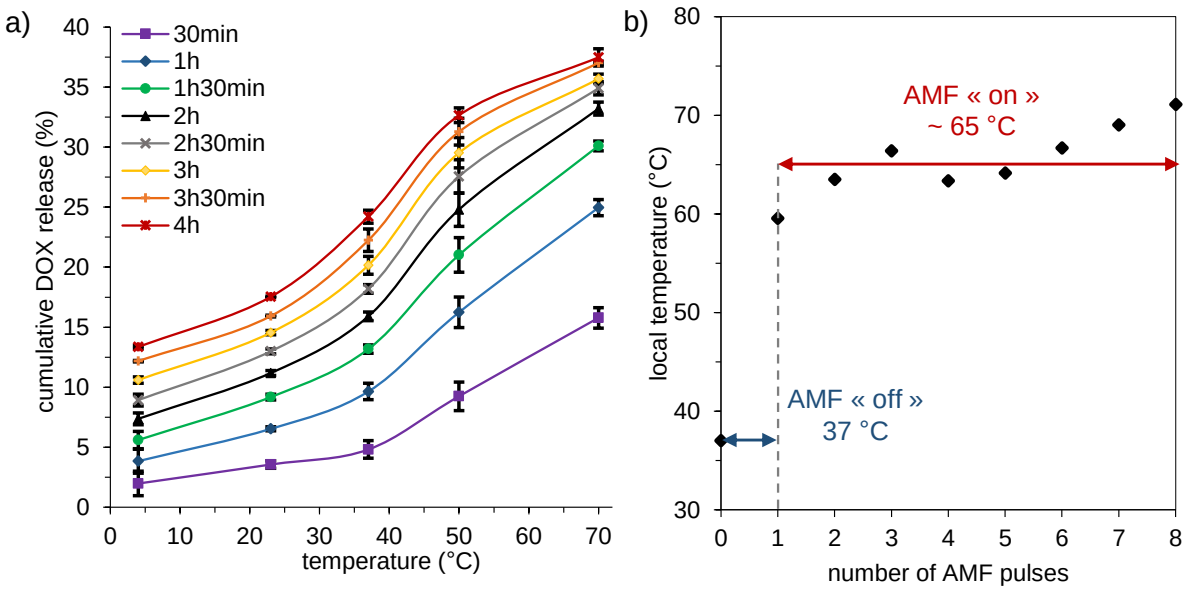

Figure 8. a) Cumulative DOX release profile (%) versus incubation temperature of DOX-MagNanoGels-37.5 wt% ([Fe] = 8.35mM) at pH 7.5 (0.1 M hepes buffer sodium) by controlling the temperature of the sample (water bath) at different times. b) Estimation of the local temperature variation near the surface of MNPs at pH 7.5 after applying different AMF pulses (335 kHz, 9 mT, 30 min).

3.6 Intracellular DOX Release

The cellular capture of MagNanoGels-37.5 wt%, DOX-MagNanoGels-37.5 wt% and free DOX, as well as the remote DOX intracellular release triggered by AMF were investigated in PC-3 cancer cells (Human Prostatic Cancer Cell lines), foreseeing future cancer therapy application.

3.6.1 Cellular Internalization and Cytotoxicity of MagNanoGels and DOX-MagNanoGels

After 2 hours incubation of the cells with the MagNanoGels, cellular iron load was measured by single-cell magnetophoresis. MagNanoGels and DOX-MagNanoGels were equally captured by PC-3 cancer cells, with an important iron load saturating with the extracellular concentration at about 15 pg of iron per cell (Figure 9 a). The presence of DOX within the nanogels thus does not interfere with their cellular internalization. Remarkably, both DOX-MagNanoGels and MagNanoGels were internalized as efficiently as free nanoparticles (MNPs). Supplementary Figures S11 and S12 show the cellular localization of MagNanoGels and DOX-MagNanoGels respectively, right after incubation, 4 hours after and 24 hours after (only for DOX-MagNanoGels). For both, right after incubation, the MagNanoGels, labeled with rhodamine covalently bonded to the gels (RHO in red), were mostly found on the cell membranes (see the 3D reconstructed z-profile in Figure S11). By contrast, 4 hours after, they were clearly internalized and localized as small intracellular dots identified as endosomes (Figure S11). For DOX-MagNanoGels, the doxorubicin, encapsulated in MagNanoGels (DOX in green), and the rhodamine, covalently bonded to MagNanoGels (RHO in red), were clearly associated with the MagNanoGels (colocalized with RHO) right after incubation. It was partly delivered to the nuclei 4-hours and 24-hours after incubation, but with still a large proportion of green dots associated to the RHO-MagNanoGels (Figure S12).

The metabolic activity (Alamar Blue assay) of PC-3 cancer cells was measured 24 hours after the end of the 2 hours incubation with free DOX, MagNanoGels and DOX-MagNanoGels. For all experiments, cell samples were thermostated at 37 °C. First, MagNanoGels (without DOX) have high cell viability, proving that MagNanogels are not toxic at an iron concentration from 0.5 to 4.2 mM (Figure 9b). Second, viability was more impacted when cancer cells were incubated with DOX-MagNanoGels than with free DOX at a concentration range of 4 – 32 μM.

This demonstrates that MagNanoGels vectorize DOX intracellularly better than the molecule alone. It is confirmed by the confocal images of Figure 10, as detailed in the next paragraph.

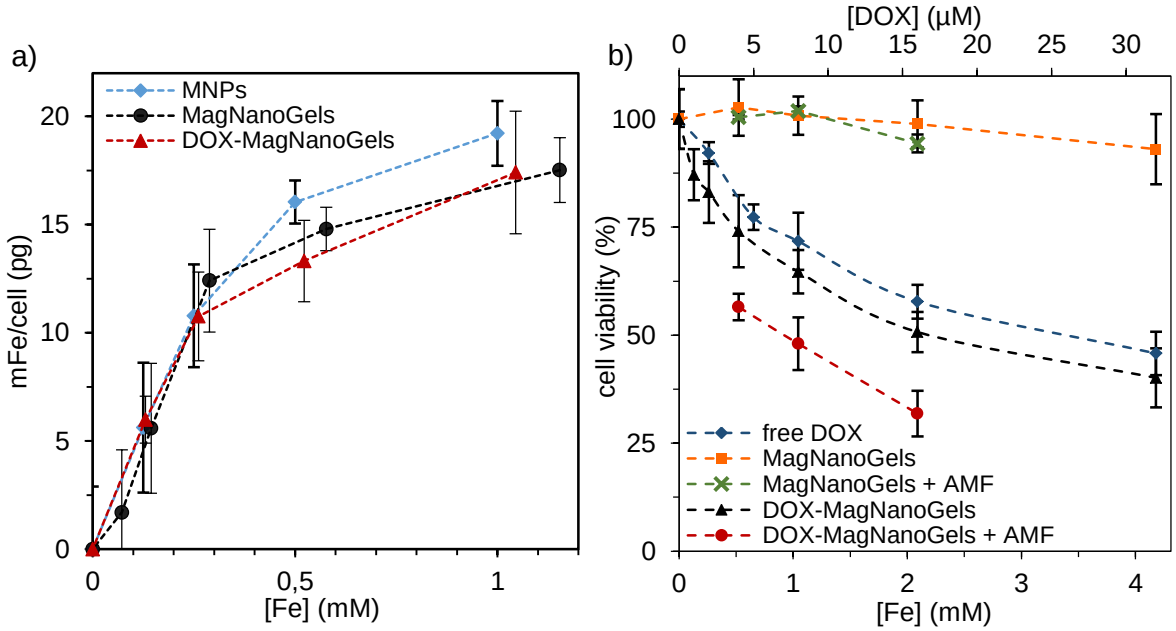

Figure 9. a) Iron load per cell after a 2-hours incubation with MagNanoGels and DOX-MagNanoGels from [Fe] = 0.13 to 1.2 mM, measured by single-cell magnetophoresis. b) Cell viability of PC-3 cells (normalized by control cells) incubated for 2 h with free DOX, MagNanoGels and DOX-MagNanoGels with and without AMF (AMF was applied 2 hours after the end of incubation, and for 2 hours, at 471 kHz, 18 mT; 14.4 $kA.m^{-1}$). The x-axis of iron concentration [Fe] from 0.5 to 4.2 mM corresponds to an equivalent DOX concentration [DOX] from 4 to 32 µM for the DOX-MagNanoGels. For MagNanoGels, only the iron concentration axis applies. For free DOX, only the DOX concentration axis applies.

3.6.2 Intracellular Remote DOX Release from MagNanoGels under AMF

Cell viability was finally assessed after 2 hours of AMF application (Figure 9b, condition DOX-MagNanoGels + AMF compared to DOX-MagNanoGels). The viability was significantly

lowered after AMF stimulation. As a result, the half maximal inhibitory concentration – IC_{50} of free DOX, DOX-MagNanoGels without and with AMF were respectively 26 µM, 19 µM and 8 µM. Very importantly, during all AMF experiments, no macroscopic heating was measured. Besides, a control experiment was performed, where cells loaded with MagNanoGels without DOX where also submitted to the 2-hours AMF stimulation (Figure 9b, condition MagNanoGels + AMF). In this case, viability was not affected and was similar to the one of the control (100%). This proves that there is no cell death by simple heating, confirming the athermal conditions. Thus, cancer cell death is enhanced under AMF due to an increase of DOX release from the MagNanoGels, as on batch experiments; and the localized heating of MNPs contained into nanogels and generated under AMF is high enough to remotely trigger DOX release, but not sufficient to destroy by itself the cancer cells.

The intracellular DOX releases with and without AMF were then tracked by confocal microscopy (Figure 10). All images were taken 4 hours after the end of cells incubation (at [DOX] = 4 and 8 µM).

When cells were incubated with DOX-MagNanoGels (Figures 10a and 10b), some DOX localizes within the nucleus, but some remains in the cytoplasm, as small dots colocalized with the fluorescence of the RHO-MagNanoGels (linked covalently to RHO). The intracellular delivery of both DOX and RHO is higher at the incubation condition [DOX] = 8 µM than at [DOX] = 4 µM. Images of cells incubated with free DOX are also shown in Figure 10c. In this case, all the drug is found in the nucleus. Of note, the amount of DOX provided by MagNanoGels to the cell nuclei seems slightly higher than that internalized by the free DOX.

The most striking observation concerns the nuclei DOX fluorescence in cancer cells incubated with DOX-MagNanogels and submitted to AMF (Figures 10a and 10b). It is clearly increased by

the application of AMF. To quantify these effects, we next measured the average fluorescence intensity in a circular area contained within the nucleus and processed the pictures with ImageJ software (Figure 10d). First, it confirms that the fluorescence nuclear intensity of DOX is higher for the cells incubated with DOX-MagNanoGels than for those incubated with free DOX, in agreement with the higher cytotoxicity of DOX-MagNanoGels compared to free DOX. Second, it clearly demonstrates the enhanced DOX nuclear delivery triggered by AMF.

Taken together, these cell studies demonstrate that the MagNanoGels allow better delivery of DOX inside the cells, thus enhancing DOX cytotoxicity; and that AMF triggers a better release, enhancing even further cytotoxicity. These results support the possibility of initiating a chemotherapeutic treatment via an athermal magnetic hyperthermia strategy. This is particularly promising to limit the adverse effects of chemotherapy on surrounding normal tissues. Moreover, the MNPs, contained in the nanogels, would allow to visualize tumors by Magnetic Resonance Imaging **(**MRI), thus these magnetic nanogels could be used as a polymer-based theranostic platform for cancer therapy afterwards[47].

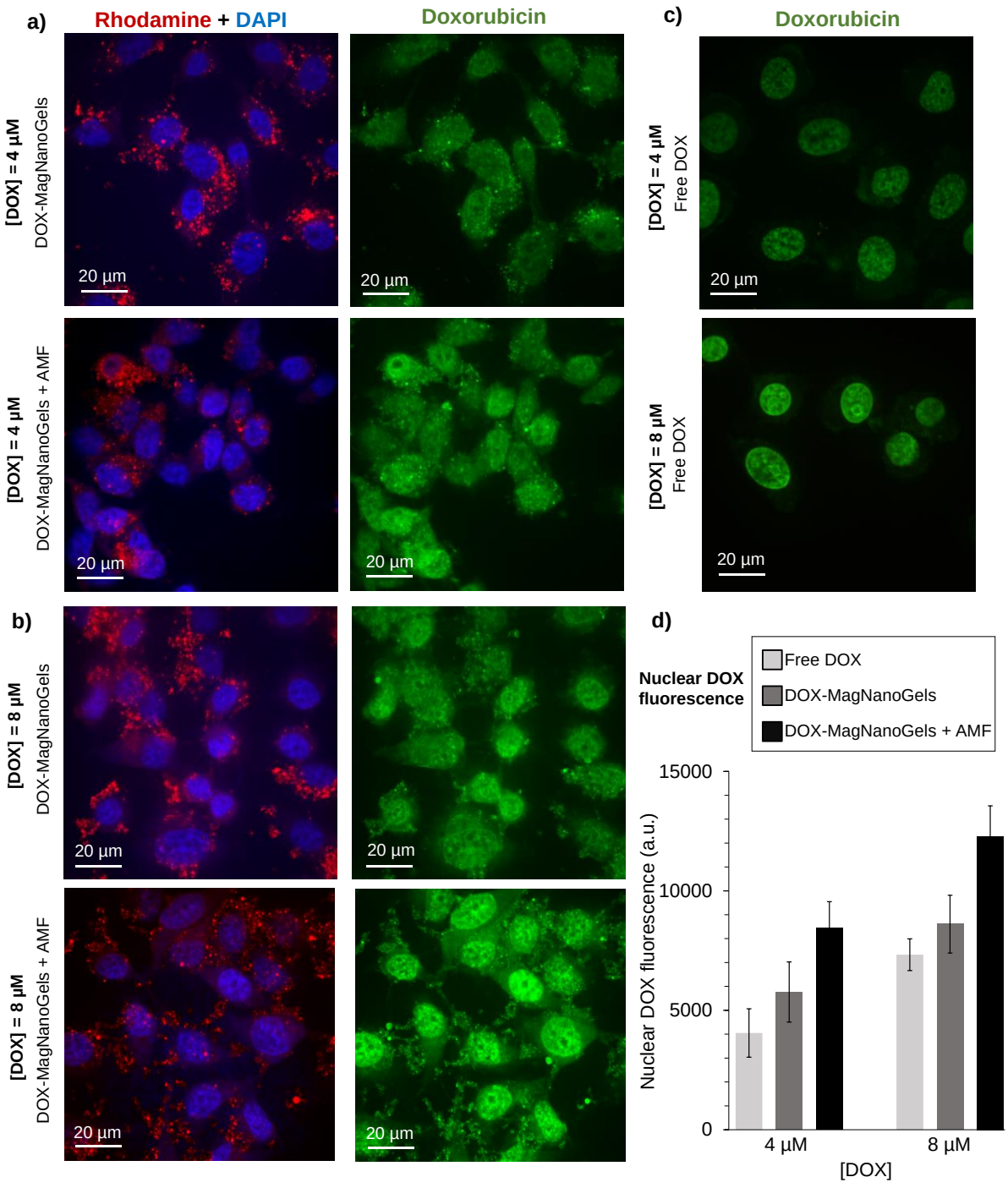

Figure 10. Confocal fluorescence imaging PC-3 cancer cells after 2 hours incubation of DOX-MagNanoGels (a, b). Incubation was performed at a) [DOX] = 4 µM or b) 8 µM. Cells were fixed 4 hours after the end of the incubation. During this 4-hours period, cells were submitted to

a 2-hours cycle of AMF (condition + AMF, bottom image), or left at 37°C in the incubator (top image). For comparison, c) cells incubated for 2 hours with free DOX are also shown for the two incubation conditions: [DOX] = 4 µM and 8 µM. Fluorescence was collected in the blue channel (DAPI, excitation at 405 nm), in the red channel (Rhodamine – RHO, excitation at 561 nm) or in the green channel (Doxorubicin – DOX, excitation at 488 nm). d) For all conditions, fluorescence was quantified in the nuclear region for DOX fluorescence (green) and averaged measures are represented (n>16, error bars represent the standard deviation).

CONCLUSIONS

In summary, biocompatible, multi-responsive magnetic nanogels were synthetized by aqueous precipitation radical co-polymerization and post-assembly with MNPs. MagNanoGels, containing 37.5 wt% of MNPs, have a high drug loading efficiency (60 %) and their swelling-deswelling transition, as well as drug release can be controlled either by internal (pH) and external (temperature, alternative magnetic field) stimuli. Indeed, the release of DOX can be enhanced by rising the temperature (17 vs. 36 % at 23 and 70 °C respectively), decreasing the pH (24 vs. 96 % at pH 7.5 and 5.0 respectively) and by applying AMF (24 vs. 47 % without and with AMF respectively). We demonstrated that these nanogels are excellent nanocarriers for enhancing the internalization of DOX inside cancer cells and, most important, that it is possible to trigger intracellularly and remotely DOX release under AMF by "hot spot" effect, thus enhancing DOX efficiency in terms of cytotoxicity. Thus, cancer cell viability could be reduced from 51 to 32 % by applying AMF to DOX-MagNanoGels inside the cells. Because AMF itself is non-toxic and can deeply penetrate into human tissues, such nanocarriers could be a promising drug delivery system strategy, which could be applied to other hydrophilic drugs. Furthermore,

the presence of magnetic particles opens the possibility to combine the remotely trigger drug delivery ability with real-time imaging (MRI) and magnetic targeting for a theranostic cancer therapy strategy with a single nanocarrier.

ASSOCIATED CONTENT

Supporting Information

The Supporting Information is available free of charge on the ACS Publications website at DOI: 10.1021/acsami.7b06553

1. NanoGels characterization: Potentiometric and conductimetric titrations of carboxylic acid units (-COOH) inside nanogels. TEM images and size distribution (DLS) of NanoGels. **2. Magnetic nanoparticles characterization:** TEM image, size distribution and magnetization curve of MNPs. **3. MagNanoGels characterization:** Thermogravimetric analysis. Temperature and diameter (TEM, cryo-TEM) measurements during AMF experiments. **4. Encapsulation and release of doxorubicin:** calibration curves of DOX absorption (485 nm) versus the DOX concentration of standard solutions. Cumulative DOX release profile (%) versus time at 25 °C, pH 7.5 without and with AMF at different frequencies (335 and 471 kHz). **5. Cells studies:** confocal microscopy images of intracellular internalization of free DOX and DOX-loaded RHO-MagNanoGels.

AUTHOR INFORMATION

Corresponding Author

*Email: christine.menager@upmc.fr / claire.wilhelm@univ-paris-diderot.fr

ORCID

Esther Cazares-Cortes: 0000-0002-2215-0291

Ana Espinosa : 0000-0002-5626-6129

Claire Wilhelm : 0000-0001-7024-9627

Christine Ménager : 0000-0002-4080-3508

Notes

The authors declare no competing financial interests.

ACKNOWLEDGMENT

TEM images were taken at IMPC (Institut des Matériaux de Paris-Centre), FR 2482. Cryo-TEM images were taken at IMPMC (Institut de Minéralogie, de Physique des Matériaux et de Cosmochimie), at UPMC (Université Pierre et Marie Curie), Paris. We kindly thank Frédéric Gélébart for technical support with Magnetherm device and Delphine Talbot for TGA characterization.

ABBREVIATIONS

AMF, alternative magnetic field

Cryo-TEM, Cryogenic-Transmission Electronic Microscopy

CLSM, Confocal laser scanning microscopy

DDS, Drug Delivery System

DLS, dynamic light scattering

DOX, doxorubicin

IC_{50}, Half maximal inhibitory concentration

KPS, potassium persulfate

MAA, methacrylic acid

MEO_2MA, di(ethylene glycol) methyl ether methacrylate (Mn = 188.22g.mol^{-1})

MNPs, magnetic nanoparticles

NTA, nanoparticle tracking analysis

Oe, Œrsted (unit of a magnetic field H)

OEGDA, poly(ethylene glycol) diacrylate (Mn = 250g.mol^{-1})

OEGMA, poly(ethylene glycol) methyl ether methacrylate (Mn = 500g.mol^{-1})

PC-3, human prostate cancer cells

SLP, Specific Loss Power

SQUID, Superconducting Quantum Interference Device

TEM, Transmission Electronic Microscopy

TGA, ThermoGravimetric Analysis

VSM, Vibrating Sample Magnetometer

VPTT, Volume Phase Temperature Transition

REFERENCES

(1) Brazel, C. S. Magnetothermally-Responsive Nanomaterials: Combining Magnetic Nanostructures and Thermally-Sensitive Polymers for Triggered Drug Release. *Pharm. Res.* **2009**, *26* (3), 644–656.

(2) Luk, B. T.; Zhang, L. Current Advances in Polymer-Based Nanotheranostics for Cancer Treatment and Diagnosis. *ACS Appl. Mater. Interfaces* **2014**, *6* (24), 21859–21873.

(3) Kaur, S.; Prasad, C.; Balakrishnan, B.; Banerjee, R. Trigger Responsive Polymeric Nanocarriers for Cancer Therapy. *Biomater Sci* **2015**, *3* (7), 955–987.

(4) Bergueiro, J.; Calderón, M. Thermoresponsive Nanodevices in Biomedical Applications: Thermoresponsive Nanodevices in Biomedical Applications …. *Macromol. Biosci.* **2015**, *15* (2), 183–199.

(5) Molina, M.; Asadian-Birjand, M.; Balach, J.; Bergueiro, J.; Miceli, E.; Calderón, M. Stimuli-Responsive Nanogel Composites and Their Application in Nanomedicine. *Chem Soc Rev* **2015**.

(6) Yang, H.; Wang, Q.; Huang, S.; Xiao, A.; Li, F.; Gan, L.; Yang, X. Smart PH/Redox Dual-Responsive Nanogels for On-Demand Intracellular Anticancer Drug Release. *ACS Appl. Mater. Interfaces* **2016**, *8* (12), 7729–7738.

(7) Álvarez-Bautista, A.; Duarte, C. M. M.; Mendizábal, E.; Katime, I. Controlled Delivery of Drugs through Smart PH-Sensitive Nanohydrogels for Anti-Cancer Therapies: Synthesis, Drug Release and Cellular Studies. *Des. Monomers Polym.* **2016**, *19* (4), 319–329.

(8) Li, Z.; Ye, E.; David; Lakshminarayanan, R.; Loh, X. J. Recent Advances of Using Hybrid Nanocarriers in Remotely Controlled Therapeutic Delivery. *Small* **2016**, *12* (35), 4782–4806.

(9) Regmi, R.; Bhattarai, S. R.; Sudakar, C.; Wani, A. S.; Cunningham, R.; Vaishnava, P. P.; Naik, R.; Oupicky, D.; Lawes, G. Hyperthermia Controlled Rapid Drug Release from Thermosensitive Magnetic Microgels. *J. Mater. Chem.* **2010**, *20* (29), 6158.

(10) Hu, Y.; Liu, W.; Wu, F. Novel Multi-Responsive Polymer Magnetic Microgels with Folate or Methyltetrahydrofolate Ligand as Anticancer Drug Carriers. *RSC Adv.* **2017**, *7* (17), 10333–10344.

(11) Indulekha, S.; Arunkumar, P.; Bahadur, D.; Srivastava, R. Dual Responsive Magnetic Composite Nanogels for Thermo-Chemotherapy. *Colloids Surf. B Biointerfaces* **2017**, *155*, 304–313.

(12) Brulé, S.; Levy, M.; Wilhelm, C.; Letourneur, D.; Gazeau, F.; Ménager, C.; Le Visage, C. Doxorubicin Release Triggered by Alginate Embedded Magnetic Nanoheaters: A Combined Therapy. *Adv. Mater.* **2011**, *23* (6), 787–790.

(13) Deka, S. R.; Quarta, A.; Di Corato, R.; Riedinger, A.; Cingolani, R.; Pellegrino, T. Magnetic Nanobeads Decorated by Thermo-Responsive PNIPAM Shell as Medical Platforms for the Efficient Delivery of Doxorubicin to Tumour Cells. *Nanoscale* **2011**, *3* (2), 619–629.

(14) Kakwere, H.; Leal, M. P.; Materia, M. E.; Curcio, A.; Guardia, P.; Niculaes, D.; Marotta, R.; Falqui, A.; Pellegrino, T. Functionalization of Strongly Interacting Magnetic Nanocubes with (Thermo)Responsive Coating and Their Application in Hyperthermia and Heat-Triggered Drug Delivery. *ACS Appl. Mater. Interfaces* **2015**, *7* (19), 10132–10145.

(15) Sanson, C.; Diou, O.; Thévenot, J.; Ibarboure, E.; Soum, A.; Brûlet, A.; Miraux, S.; Thiaudière, E.; Tan, S.; Brisson, A.; Dupuis, V.; Sandre, O.; Lecommandoux, S.

Doxorubicin Loaded Magnetic Polymersomes: Theranostic Nanocarriers for MR Imaging and Magneto-Chemotherapy. *ACS Nano* **2011**, *5* (2), 1122–1140.
(16) Griffete, N.; Fresnais, J.; Espinosa, A.; Wilhelm, C.; Bée, A.; Ménager, C. Design of Magnetic Molecularly Imprinted Polymer Nanoparticles for Controlled Release of Doxorubicin under an Alternative Magnetic Field in Athermal Conditions. *Nanoscale* **2015**.
(17) Riedinger, A.; Guardia, P.; Curcio, A.; Garcia, M. A.; Cingolani, R.; Manna, L.; Pellegrino, T. Subnanometer Local Temperature Probing and Remotely Controlled Drug Release Based on Azo-Functionalized Iron Oxide Nanoparticles. *Nano Lett.* **2013**, *13* (6), 2399–2406.
(18) Guisasola, E.; Baeza, A.; Talelli, M.; Arcos, D.; Moros, M.; de la Fuente, J. M.; Vallet-Regí, M. Magnetic-Responsive Release Controlled by Hot Spot Effect. *Langmuir* **2015**, *31* (46), 12777–12782.
(19) Hua, X.; Yang, Q.; Dong, Z.; Zhang, J.; Zhang, W.; Wang, Q.; Tan, S.; Smyth, H. D. C. Magnetically Triggered Drug Release from Nanoparticles and Its Applications in Anti-Tumor Treatment. *Drug Deliv.* **2017**, *24* (1), 511–518.
(20) Lutz, J.-F.; Andrieu, J.; Üzgün, S.; Rudolph, C.; Agarwal, S. Biocompatible, Thermoresponsive, and Biodegradable: Simple Preparation of "All-in-One" Biorelevant Polymers. *Macromolecules* **2007**, *40* (24), 8540–8543.
(21) Cai, T.; Marquez, M.; Hu, Z. Monodisperse Thermoresponsive Microgels of Poly(Ethylene Glycol) Analogue-Based Biopolymers. *Langmuir* **2007**, *23* (17), 8663–8666.
(22) Lutz, J.-F. Polymerization of Oligo(Ethylene Glycol) (Meth)Acrylates: Toward New Generations of Smart Biocompatible Materials. *J. Polym. Sci. Part Polym. Chem.* **2008**, *46* (11), 3459–3470.
(23) Hu, Z.; Cai, T.; Chi, C. Thermoresponsive Oligo(Ethylene Glycol)-Methacrylate- Based Polymers and Microgels. *Soft Matter* **2010**, *6* (10), 2115–2123.
(24) Lutz, J.-F. Thermo-Switchable Materials Prepared Using the OEGMA-Platform. *Adv. Mater.* **2011**, *23* (19), 2237–2243.
(25) Yang, H.; Wang, Q.; Chen, W.; Zhao, Y.; Yong, T.; Gan, L.; Xu, H.; Yang, X. Hydrophilicity/Hydrophobicity Reversable and Redox-Sensitive Nanogels for Anticancer Drug Delivery. *Mol. Pharm.* **2015**, *12* (5), 1636–1647.
(26) Massart, R. Preparation of Aqueous Magnetic Liquids in Alkaline and Acidic Media. *IEEE Trans. Magn.* **1981**, *17* (2), 1247–1248.
(27) Lefebure, S.; Dubois, E.; Cabuil, V.; Neveu, S.; Massart, R. Monodisperse Magnetic Nanoparticles: Preparation and Dispersion in Water and Oils. *J. Mater. Res.* **1998**, *13* (10), 2975–2981.
(28) Boularas, M.; Gombart, E.; Tranchant, J.-F.; Billon, L.; Save, M. Design of Smart Oligo(Ethylene Glycol)-Based Biocompatible Hybrid Microgels Loaded with Magnetic Nanoparticles. *Macromol. Rapid Commun.* **2015**, *36* (1), 79–83.
(29) Hoare, T.; Pelton, R. Functional Group Distributions in Carboxylic Acid Containing Poly(*N* -Isopropylacrylamide) Microgels. *Langmuir* **2004**, *20* (6), 2123–2133.
(30) Hoare, T.; Pelton, R. Titrametric Characterization of PH-Induced Phase Transitions in Functionalized Microgels. *Langmuir* **2006**, *22* (17), 7342–7350.
(31) Bacri, J.-C.; Perzynski, R.; Salin, D.; Cabuil, V.; Massart, R. Magnetic Colloidal Properties of Ionic Ferrofluids. *J. Magn. Magn. Mater.* **1986**, *62* (1), 36–46.

(32) Borukhov, I.; Andelman, D.; Borrega, R.; Cloitre, M.; Leibler, L.; Orland, H. Polyelectrolyte Titration: Theory and Experiment. *J. Phys. Chem. B* **2000**, *104* (47), 11027–11034.
(33) Boularas, M.; Deniau-Lejeune, E.; Alard, V.; Tranchant, J.-F.; Billon, L.; Save, M. Dual Stimuli-Responsive Oligo(Ethylene Glycol)-Based Microgels: Insight into the Role of Internal Structure in Volume Phase Transitions and Loading of Magnetic Nanoparticles to Design Stable Thermoresponsive Hybrid Microgels. *Polym Chem* **2016**, *7* (2), 350–363.
(34) Fortin, J.-P.; Wilhelm, C.; Servais, J.; Ménager, C.; Bacri, J.-C.; Gazeau, F. Size-Sorted Anionic Iron Oxide Nanomagnets as Colloidal Mediators for Magnetic Hyperthermia. *J. Am. Chem. Soc.* **2007**, *129* (9), 2628–2635.
(35) Fauconnier, N.; Bée, A.; Roger, J.; Pons, J. N. Synthesis of Aqueous Magnetic Liquids by Surface Complexation of Maghemite Nanoparticles. *J. Mol. Liq.* **1999**, *83* (1–3), 233–242.
(36) Smeets, N. M. B.; Hoare, T. Designing Responsive Microgels for Drug Delivery Applications. *J. Polym. Sci. Part Polym. Chem.* **2013**, *51* (14), 3027–3043.
(37) Ganta, S.; Devalapally, H.; Shahiwala, A.; Amiji, M. A Review of Stimuli-Responsive Nanocarriers for Drug and Gene Delivery. *J. Controlled Release* **2008**, *126* (3), 187–204.
(38) Janssen, M.; Crommelin, D.; Storm, G.; Hulshoff, A. Doxorubicin Decomposition on Storage. Effect of PH, Type of Buffer and Liposome Encapsulation. *Int. J. Pharm.* **1985**, *23* (1), 1–11.
(39) Xiong, W.; Wang, W.; Wang, Y.; Zhao, Y.; Chen, H.; Xu, H.; Yang, X. Dual Temperature/PH-Sensitive Drug Delivery of Poly(N-Isopropylacrylamide-Co-Acrylic Acid) Nanogels Conjugated with Doxorubicin for Potential Application in Tumor Hyperthermia Therapy. *Colloids Surf. B Biointerfaces* **2011**, *84* (2), 447–453.
(40) Oliveira, H.; Pérez-Andrés, E.; Thevenot, J.; Sandre, O.; Berra, E.; Lecommandoux, S. Magnetic Field Triggered Drug Release from Polymersomes for Cancer Therapeutics. *J. Controlled Release* **2013**, *169* (3), 165–170.
(41) Jaiswal, M. K.; De, M.; Chou, S. S.; Vasavada, S.; Bleher, R.; Prasad, P. V.; Bahadur, D.; Dravid, V. P. Thermoresponsive Magnetic Hydrogels as Theranostic Nanoconstructs. *ACS Appl. Mater. Interfaces* **2014**, *6* (9), 6237–6247.
(42) Vihola, H.; Laukkanen, A.; Valtola, L.; Tenhu, H.; Hirvonen, J. Cytotoxicity of Thermosensitive Polymers Poly(N-Isopropylacrylamide), Poly(N-Vinylcaprolactam) and Amphiphilically Modified Poly(N-Vinylcaprolactam). *Biomaterials* **2005**, *26* (16), 3055–3064.
(43) Wadajkar, A. S.; Koppolu, B.; Rahimi, M.; Nguyen, K. T. Cytotoxic Evaluation of N-Isopropylacrylamide Monomers and Temperature-Sensitive Poly(N-Isopropylacrylamide) Nanoparticles. *J. Nanoparticle Res.* **2009**, *11* (6), 1375–1382.
(44) Bianco-Peled, H.; Gryc, S. Binding of Amino Acids to "Smart" Sorbents: Where Does Hydrophobicity Come into Play? *Langmuir* **2004**, *20* (1), 169–174.
(45) Lutz, J.-F. Polymerization of Oligo(Ethylene Glycol) (Meth)Acrylates: Toward New Generations of Smart Biocompatible Materials. *J. Polym. Sci. Part Polym. Chem.* **2008**, *46* (11), 3459–3470.
(46) Brites, C. D. S.; Lima, P. P.; Silva, N. J. O.; Millán, A.; Amaral, V. S.; Palacio, F.; Carlos, L. D. A Luminescent Molecular Thermometer for Long-Term Absolute Temperature Measurements at the Nanoscale. *Adv. Mater.* **2010**, *22* (40), 4499–4504.
(47) Luk, B. T.; Zhang, L. Current Advances in Polymer-Based Nanotheranostics for Cancer Treatment and Diagnosis. *ACS Appl. Mater. Interfaces* **2014**, *6* (24), 21859–21873.

Abstract Graphic